2010

The off-axis pyroelectric effect observed for lithium tetraborate

J. Ketsman

D. Wooten

Jie Xiao

Ya. B. Losovyj

Ya. V. Burak

See next page for additional authors

Authors
J. Ketsman, D. Wooten, Jie Xiao, Ya. B. Losovyj, Ya. V. Burak, V. T. Adamiv, A. Sokolov, J. Petrosky, J. McClory, and P. A. Dowben

Physics Letters A 374 (2010) 891–895

Contents lists available at ScienceDirect

Physics Letters A

www.elsevier.com/locate/pla

The off-axis pyroelectric effect observed for lithium tetraborate

I. Ketsman [a], D. Wooten [b], Jie Xiao [a], Ya.B. Losovyj [a,c], Ya.V. Burak [d], V.T. Adamiv [d], A. Sokolov [a], J. Petrosky [b], J. McClory [b], P.A. Dowben [a,*]

[a] Dept. of Physics and Astronomy and the Nebraska Center for Materials and Nanoscience, University of Nebraska-Lincoln, PO Box 880111, Lincoln, NE 68588-0111, USA
[b] Air Force Institute of Technology, 2950 Hobson Way, Wright Patterson Air Force Base, OH 45433-7765, USA
[c] J. Bennett Johnston Sr. Center for Advanced Microstructures and Devices, Louisiana State University, 6980 Jefferson Highway, Baton Rouge, LA 70806, USA
[d] Institute of Physical Optics, 23 Dragomanov Street, Lviv 79005, Ukraine

ARTICLE INFO

Article history:
Received 3 September 2009
Received in revised form 30 November 2009
Accepted 4 December 2009
Available online 9 December 2009
Communicated by R. Wu

Keywords:
Pyroelectric effect
Lithium tetraborate
Coupled order parameters

ABSTRACT

We find a pyroelectric current along the ⟨110⟩ direction of stoichiometric $Li_2B_4O_7$ so that the pyroelectric coefficient is nonzero but roughly 10^{-3} smaller than along the ⟨001⟩ direction of spontaneous polarization. Abrupt decreases in the pyroelectric coefficient along the ⟨110⟩ direction can be correlated with anomalies in the elastic stiffness C_{33}^{D} contributing to concept that the pyroelectric coefficient is not simply a vector but has qualities of a tensor, as expected. The time dependent surface photovoltaic charging suggests that an inverse piezoelectric effect occurs at the (110) surface but not the (100) surface. Both effects along the ⟨110⟩ direction or at the (110) surface are distinct the conventional as a bulk pyroelectric effect.

1. Introduction

The study of pyroelectricity has a long and rich history [1], but there have been good reasons to suspect for more than half a century [2] that the general models of pyroelectricity tend to be simplistic. Pyroelectricity is usually measured as a current that occurs with changing temperature along the direction of spontaneous polarization [1–4]. It is also important to note that all pyroelectric materials are piezoelectric, because the necessary spontaneous polarization only occurs in materials with a unique polar axis [2,3]. For a piezoelectric material we expect that the charge density D_i is related to the stress X_{jk} by [2,3]:

$$D_i = d_{ijk} X_{jk} \tag{1}$$

where the piezoelectric coefficients d_{ijk} form a third rank tensor. We should be able to alter the surface charge density D_i by applying an electric field as the strain is related to the applied electric field $\underline{\mathbf{E}}$ by:

$$x_{ij} = d_{kij} \underline{E}_k \tag{2}$$

and of course stress is related to strain by Hooke's law. The pyroelectric effect should in fact be a tensor because the surface charge density D_i, induced by a change in temperature T, is also related to the change in static polarization $P_{S,i}$, this, in turn is related to the pyroelectric coefficient p_i:

$$D_i = \Delta P_{S,i} = \frac{dP_{S,i}}{dT} \Delta T = p_i \Delta T. \tag{3}$$

From Eqs. (1) and (2), with changes in temperature, there is an expected anisotropy of the electric constants and the resulting "stress" with temperature, particularly in a noncubic pyroelectric crystal [2]. Although the pyroelectric coefficient is generally treated as a vector [2,3], there is implied tensor character (character higher than a first order tensor from the coupling to the stress–strain tensor and the accompanying tensor character of the piezoelectric effect). Indeed it is recognized that there is a secondary pyroelectric effect that can occur if the pyroelectric crystal is allowed to deform along directions other than the polar direction [2]. This makes Eq. (3), relating the surface charge density D_i to the pyroelectric coefficients p_i, over-simplistic, as this effort conclusively demonstrates for lithium tetraborate ($Li_2B_4O_7$). Prior optical studies have provided some indications of an off axis pyroelectric effect along crystal directions orthogonal to the polar axis of some translucent pyroelectric crystals [5], but not for lithium tetraborate.

Lithium tetraborate ($Li_2B_4O_7$) is a tetragonal crystal of space group of $I4_1cd$ with 104 atoms per unit cell [6–9] with an appreciable pyroelectric coefficient in the region of 100 to 250 K [10,11]. As the tetragonal crystal lattice of lithium tetraborate is the result of stretching a cubic lattice along one lattice vector, so that the unit cell is a rectangular prism with a square base (a by a, $a = 9.48$ Å) and height ($c = 10.29$ Å, which differs from a) [6–9]. The ⟨110⟩ and ⟨100⟩ crystal directions are orthogonal to the polar

* Corresponding author.
E-mail address: pdowben@unl.edu (P.A. Dowben).

0375-9601/$ – see front matter
doi:10.1016/j.physleta.2009.12.012

⟨001⟩ direction for the tetragonal crystal lattice and thus candidates for the study of an off-axis pyroelectric effect.

2. Experimental

The $Li_2B_4O_7$ single crystals were grown from the melt by the Czochralski technique as described elsewhere [12,13] and both the ⟨110⟩ and ⟨100⟩ crystals have been cut with a miscut of no more than 0.5°, as determined by X-ray diffraction [9]. The pyroelectric measurements along the ⟨110⟩ and ⟨100⟩ directions were performed in a manner similar to prior studies [10,11] over a range of heating rates from 0.015 to 0.4 K/s. At the lowest temperatures (50–70 K), the heating and cooling rates deviate from the linear, and these deviations have been taken into account in the analysis: variations in the heating rate from experiment to experiment were not found to significantly alter the measured pyroelectric coefficients, described below. To avoid tertiary pyroelectricity (false secondary pyroelectricity) due to uneven heating [2], the pyroelectric measurements were undertaken in a copper enclosed apparatus to ensure uniform heating and an absence of illumination. The heating and cooling was accomplished through a combination of liquid nitrogen cooling and inductive heating.

In addition, temperature dependent angle-resolved photoemission spectra were obtained using linearly polarized synchrotron light dispersed by a 3m toroidal grating monochromator [14,15], at the Center for Advanced Microstructures and Devices (CAMD) [16]. The measurements were made in an ultra-high vacuum (UHV) chamber employing a hemispherical electron analyzer with an angular acceptance of ±1°, as described elsewhere [14,15]. The photoemission experiments were undertaken with a light incidence angle of 45° with respect to the surface normal, unless stated otherwise. The photoelectrons were collected along the surface normal throughout. The photoemission was conducted over a range of temperatures from 250 to 700 K, but the binding energies are referenced to the Fermi level established at temperatures greater than 623 K, where surface charging was found to be negligible [17,18]. The location of the Fermi level was determined via angle-resolved photoemission using tantalum films in electrical contact with the samples [17,18]. The reference of the observed binding energies to the Fermi level for $Li_2B_4O_7$(110), as done here, differs from the sometimes common practice of assigning binding energies with respect to the valence band maximum for lithium borate [19]. Prior studies of lithium tetraborate also have assigned their binding energies with respect to the chemical potential or Fermi level [20]. We chose the latter convention for this investigation, i.e. citing binding energies in terms of $E - E_F$. In the photoemission experiments, after various combinations of argon ion sputtering and annealing, the surface was found to ordered, stoichiometric and free of contamination. The surface ordering was confirmed by the presence of a dispersing (E versus $k_{\|}$ dependent) band structure in angle-resolved inverse photoemission with the critical points that match the expected surface periodicity. The absence of surface contamination at the $Li_2B_4O_7$(110) surface prepared for the temperature dependent photoemission studies is evident in the photoemission spectra taken at higher photon energies [18] and from clear evidence of a light (0.42 m^*/m_e) mass image state [21] in the angle-resolved inverse photoemission. As seen in Fig. 1, the combined photoemission and inverse photoemission for the $Li_2B_4O_7$(110) surface show a density of states and band gap consistent with theoretical expectations [19]. Although the unoccupied band structure of $Li_2B_4O_7$(110) surface, mapped out in inverse photoemission, is consistent with the lattice constants of the (110) surface, reconstructions of the surface cannot be excluded. Because of the extremely dielectric nature of these crystals, low energy electron diffraction intensity versus voltage $I(V)$ surface structural analysis was not possible in the temperature range where the pyroelectric currents were most evident (well below room temperature).

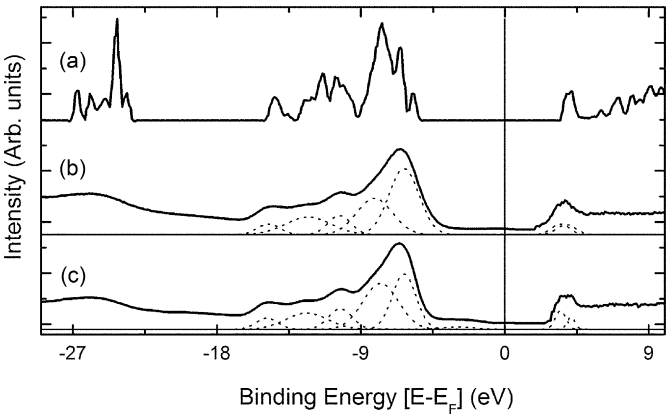

Fig. 1. The combined experimental photoemission and inverse photoemission results for bulk $Li_2B_4O_7$ taken at 623 K are compared with theory: (a) the theoretical density of states of solid $Li_2B_4O_7$ abstracted from the work of Islam et al. [19]; (b) combined experimental photoemission and inverse photoemission results for $Li_2B_4O_7$(110) surface, taken with the in-plane **E** vector oriented along ⟨001⟩ and (c) ⟨1$\underline{1}$0⟩. The photoemission spectra were taken at a photon energy of 56 eV with electrons collected along the surface normal, while the inverse photoemission was taken with electrons incident normal to the sample.

While the X-ray diffraction shows that the material is well oriented and single phase, point defects comprising of isolated oxygen vacancies and to a smaller extent isolated lithium vacancies, with a very small trace of Cu impurities were evident in electron paramagnetic resonance (EPR) and electron–nuclear double resonance (ENDOR), consistent with prior measurements [22,23]. These isolated point defects, amounting to between 2 and 5 ppm in total, were not sufficient to degrade the dielectric properties of our crystals, and there was insufficient current to observe any power law conductivity. Indeed very little current was generated with intense neutron irradiation of $Li_2B_4O_7$ crystals enriched to 95 at% ^{6}Li and 97.3 at% ^{10}B (isotopes with very high neutron capture cross-section) at more than 500 V applied bias, indicating very little dark current is possible in $Li_2B_4O_7$ crystal of natural abundance Li and B in the absence of irradiation or illumination, as is the case in the crystals studied here.

3. Off-axis pyroelectricity

From a family of pyroelectric current measurements, we measured along the ⟨110⟩ direction a generally negative current with increasing temperature and a mirror positive current with decreasing temperature, in the region of 70 to 250 K, in the geometry of our experiment, taken in the absence of illumination. This is the temperature region where the greatest pyroelectric currents where measured in prior studies [9,10] along the polar ⟨001⟩ direction, although the current measured here is along an orthogonal direction.

From the current and rate of change in temperature [2–4,10,11], we can extract the approximate pyroelectric coefficient along the ⟨110⟩ direction (Eq. (3)). While along the polar ⟨001⟩ direction, the pyroelectric coefficient p_i is about 125 μC/m^2 K at 120 K [11], we found that along ⟨110⟩ the pyroelectric coefficient p_i only reaches a maximal value of about 0.2 to 0.4 μC/m^2 K, as illustrated in Fig. 2. This pyroelectric coefficient p_i along the ⟨110⟩ direction is some 300 to 1000 times smaller than the conventional pyroelectric coefficient measured along the polar ⟨001⟩ lithium borate crystallographic direction and remains qualitatively similar in temperature dependence for currents measured from a range of heating and cooling rates.

As in some prior measurements [10], we found strong variations with temperature in the pyroelectric current and associated

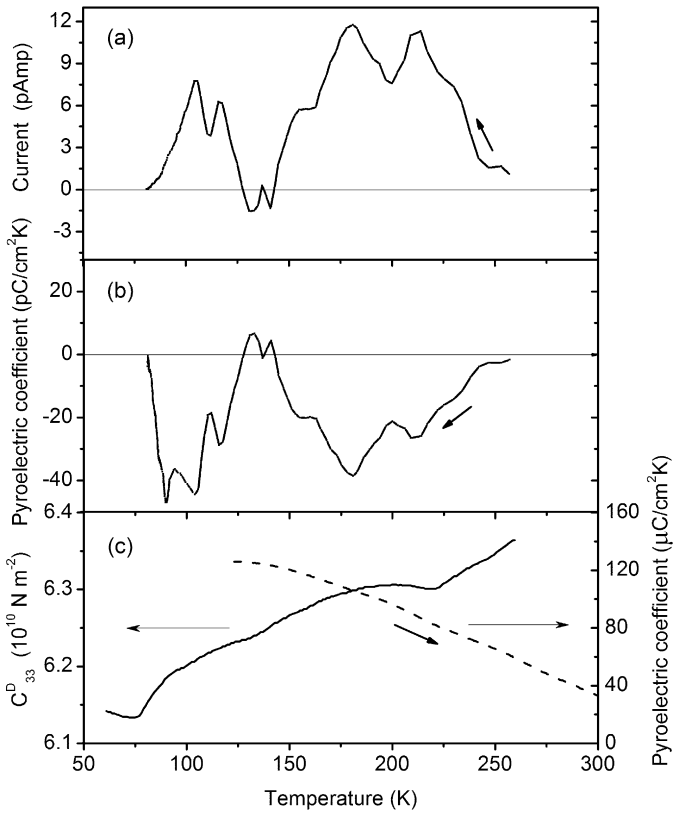

Fig. 2. (a) Pyroelectric current in the cooling cycle for the $Li_2B_4O_7$ single crystal in the ⟨110⟩ direction, at a cooling rate of roughly 0.25 degrees/s; (b) temperature dependence of the pyroelectric coefficient in the cooling cycle for the $Li_2B_4O_7$ single crystal in the ⟨110⟩ direction; (c) temperature dependence of the elastic stiffness constant C^D_{33} for the $Li_2B_4O_7$ single crystal along the polar *c*-axis (solid line), adapted from [24] and the polar ⟨001⟩ pyroelectric coefficient (dashed line) adopted from [11].

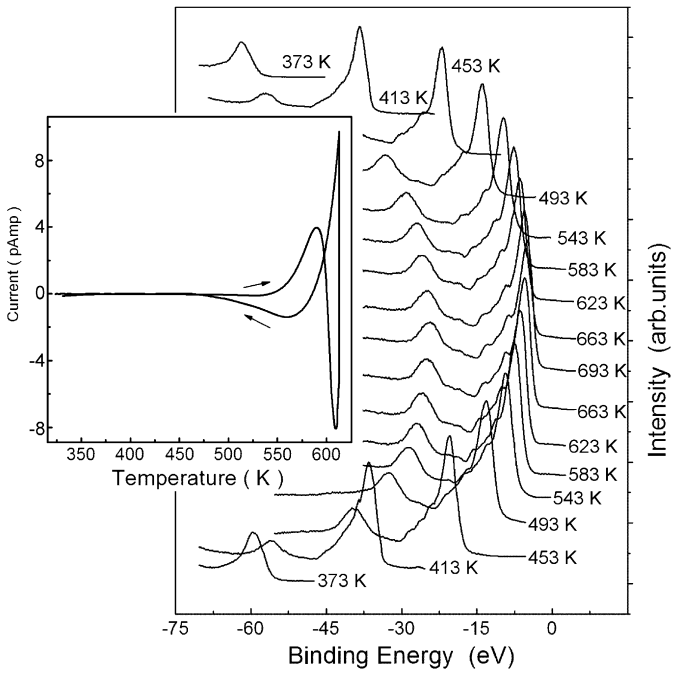

Fig. 3. The photoemission spectra from $Li_2B_4O_7$(110) surface for a succession of temperatures in a heating-cooling cycle (from bottom to top). The photoemission spectra were taken at a photon energy of 56 eV with electrons collected along the surface normal. The increase in the current magnitude, due to trapped charges, in the ⟨110⟩ direction of lithium tetraborate single crystal with increasing and decreasing temperature (as indicated) in the region of 300 to 600 K are shown in the inset.

pyroelectric coefficient, as seen in Fig. 2. Indeed, the pyroelectric coefficient does not show the same temperature dependence along the ⟨110⟩ direction as has been described [10,11] along the ⟨001⟩ direction, as indicated in Fig. 2. The fact that the measured pyroelectric currents and resulting pyroelectric coefficients along the ⟨110⟩ direction differ qualitatively from those measured along to the ⟨001⟩ polar direction [11] are compelling evidence that our measured pyroelectric coefficient is not a result a crystal miscut and therefore cannot be a projection of the expected ⟨001⟩ pyroelectric current off the polar axis.

The pyroelectric current dependence upon temperature provides dramatic relative changes in the pyroelectric coefficient along the ⟨110⟩ direction with temperature. There are large decreases in magnitude of the off-axis pyroelectric coefficient at about 80, 130 and 240 K (Fig. 1b). These temperatures are close to the observed anomalies (Fig. 1c) in the elastic stiffness observed at 75, 125 and 215 K [24]. While the elastic constant C^D_{33} decreases with decreasing temperature, reaching a minimum at about 75 K, these anomalies in the elasticity have been observed not only along the polar ⟨001⟩ direction, but also along other crystallographic directions, although significantly smaller [24]. This qualitative agreement between elastic constant anomalies and the magnitude of the off-axis pyroelectric coefficient suggests that the nonzero pyroelectric coefficient observed along the ⟨110⟩ direction is a result of anharmonic dipole oscillations or asymmetric dipole canting. The off-axis pyroelectric effect would not be expected to be as significant when the lattice is particularly soft, as may occur in the temperature regions near the elastic stiffness anomalies observed at 75, 125 and 215 K [24]. This is expected for a secondary pyroelectric effect, where temperature dependent crystal lattice deformations are permitted to occur.

4. Surface piezoelectric effects

While not all piezoelectric crystals are pyroelectrics, piezoelectric behavior is a requirement for pyroelectricity [2,3], as noted at the outset. We recognize that if there is a surface electric field, one might be able to observe a surface piezoelectric effect: this measurement is not possible using traditional transport measurements but could be observed in photoemission by exploiting the surface photovoltage effect [25–29]. These measurements cannot be directly compared with the pyroelectric measurements (Fig. 2), as illumination is required and such surface photovoltage measurements would tend to work best for a lithium borate surface that is largely defect free [30], as appears to be the case for the (110) surface based upon the observation of a highly dispersive image potential state [21] for the (110) surface, which tends to be characteristic of largely defect free surface.

At 623 K, where surface photovoltage charging was found to be negligible, the $Li_2B_4O_7$(110) exhibited a density of states that qualitatively resembles that expected from the model bulk band structure of $Li_2B_4O_7$ [13,19], as seen in Fig. 1, while the valence band maximum is in reasonable agreement with prior investigations [18–20]. Lithium tetraborate is a dielectric [11], so that in decreasing the temperature below 600 K, there is an expected increased photovoltaic charging, which in turn leads to an increase in the apparent binding energies, as seen in Fig. 3. Shifts in the photoemission spectra along the binding energy scale, due to surface charging, are temperature dependent and demonstrate hysteretic behavior in the heating-cooling cycles, as indicated in Fig. 3.

In the region of 600 K, there is a huge increase in the absolute magnitude of the current with increasing temperature and decreasing temperature. These currents in the region of 600 K are likely the result of trapped charges or charge trapping by point

defects, with the onset of decreasing or increasing conductivity, respectively, as indicated in the inset to Fig. 3, and may have little to do with the more conventional pyroelectric effect. Indeed the data suggests trapped charges are released with increasing temperature and charge trapping occurs with decreasing temperature. The fact that there are two temperature dependent current regimes, in the region of 500 to 600 K, indicates trapped charges may be associated with lithium and oxygen point defects. The charge trapping or trapped charge release may be the result of ionized defect sites of opposite charge for lithium and oxygen defects, respectively, leading to the generation of currents of opposite sign, as would be expected for oxygen and lithium vacancy defects with different charge trap potentials. The valence band features and shallow oxygen 2s core shift rigidly together, in apparent binding energies, characteristic of uniform surface photo-voltaic charging in photoemission. This is not the case for the lithium shallow core level. The lithium shallow 1s bulk core level component shifts in binding energy in "lock-step" with the valence band features, with changing temperature, but in the region of 570 to 670 K, the surface component of the lithium 1s core level shows little evidence of surface photo-voltaic charging indicating compensating negative charge collection at the (110) surface or in the vicinity of the surface lithium sites and/or there are few defects at the (110) surface. Because of the differences in apparent surface charging at the (110) surface or in the vicinity of the surface lithium sites, while unlikely, a high temperature surface pyroelectric effect in this temperature regime cannot *a priori* be excluded.

Below 500 K, the surface photo-voltaic charging is both temperature and time dependent, particularly at the (110) surface. The measured effective binding energy, for the oxygen 2s at -26.0 ± 0.6 eV ($E - E_F$) at 623 ± 5 K (Fig. 3), shows a strong decrease following an increase in temperature, below 600 K. At temperatures below 500 K, using the oxygen 2s shallow core as a benchmark this observed decrease in binding energy (and associated photovoltaic charging) can be understood as establishment of a steady state surface temperature and surface conductivity. At the (110) surface, there is not only a decrease in binding energy, but this is followed by an increase in binding energy later in time, as plotted in Fig. 4. This latter increase in binding energy later in time is observed at the (110) but not the (100) surface (Fig. 4) and this time dependent hysteresis effect is increasingly more evident at lower temperatures. As this occurs in a region where there is little or no bulk current, with changes in temperature (Fig. 3), this suggests that, while the surface photovoltage effect is initially dominated by the establishment of a steady state surface temperature and surface conductivity, the surface charge density D_i is later altered by the local electric field resulting from the surface photovoltage effect. In other words, at the (110) surface, there are changes in surface charge density D_i beyond those cause by the surface photovoltage effect alone.

While this time dependent hysteresis is likely a result of a surface piezoelectric effect, this surface piezoelectric effect does not exclude the possibility of a surface pyroelectric effect. Certainly the surface piezoelectric effect may occur at some (but not all) surfaces parallel to the direction of spontaneous polarization for lithium tetraborate, as seen from the surface photovoltage effect (Fig. 3). This too adds credence to the idea [2] that the pyroelectric coefficients p_i that include the secondary pyroelectric effect likely have some tensor character and would probably be more accurately expressed as a third order tensor p_{ijk}.

5. Summary

For the $Li_2B_4O_7$ along the ⟨110⟩ direction, a nonzero pyroelectric coefficient has been observed, far smaller than the pyroelectric coefficient along the polar direction. This off-axis pyroelectric effect cannot be reconciled with simply a projection of the polar ⟨001⟩ pyroelectric effect due to an orientational miscut, but is expected if the pyroelectric crystal is allowed to deform along directions other than the polar direction, as has been long recognized [2]. In addition, there is a large surface photovoltage charging observed at the (110) surface, which although not as large as that observed for the (100) surface, does exhibit time dependent hysteresis. In the case of the latter effect, the hysteresis increases with decreasing temperature below 500 K. In concert, these effects support the concept that pyroelectric coefficients, p_i, and the piezoelectric coefficients likely have some tensor character, so that the former should be more accurately expressed as p_{ijk}.

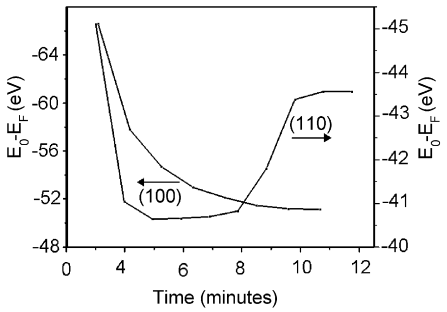

Fig. 4. The change of the magnitude of the apparent O 2s binding energy, with time, indicative of the surface photovoltaic charging of the $Li_2B_4O_7$(110) surface following a temperature increase to 390 K compared to the $Li_2B_4O_7$(100) surface following a temperature increase to 420 K.

Acknowledgements

This work was supported by the Defense Threat Reduction Agency (Grant Nos. HDTRA1-07-1-0008 and BRBAA08-I-2-0128), the NSF "QSPINS" MRSEC (DMR-0820521) at UNL and the Nebraska Research Initiative. This work was undertaken in partial fulfillment of the degree at AFIT by one author (D.W.). We thank M.W. Swinney, Shan Yang, A.T. Brant, and L.E. Halliburton for the EPR and ENDOR measurements and B. Montag, K. Nelson and D. McGregor for providing independent confirmation of the neutron irradiation conductivity. The views expressed in this article are those of the authors and do not reflect the official policy or position of the Air Force, Department of Defense or the US Government. The authors acknowledge a number of helpful conversations with Alexei Gruverman.

References

[1] S.B. Lang, Phys. Today 58 (2005) 31.
[2] J.F. Nye, Physical Properties of Crystals, Oxford University Press, Oxford, 1957, 1985, pp. 171–191, Chapter 10.
[3] D. Damjanovic, Rep. Prog. Phys. 61 (1998) 1267.
[4] Ch.G. Wu, W.L. Zhang, Y.R. Li, Zh. Liu, J. Zhu, Jpn. J. Appl. Phys. 45 (2006) 2674.
[5] V.Ya. Shur, A.L. Gruverman, S.B. Zalyuk, Ferroelectrics Piezoelectrics (1989) 81; A. Gruverman, private communication.
[6] J. Krogh-Moe, Acta Crystallogr. 15 (1962) 190.
[7] J. Krogh-Moe, Acta Crystallogr. 24 (1968) 179.
[8] M. Natarajan, R. Faggiani, I.O. Brown, Cryst. Struct. Commun. 8 (1979) 367.
[9] S.V. Radaev, L.A. Muradyan, L.F. Malakhova, Ya.V. Burak, V.I. Simonov, Kristallografiya 34 (1989) 1400.
[10] Ya.V. Burak, J. Phys. Studies 2 (1998) 62.
[11] A.S. Bhalla, L.E. Cross, R.H. Whatmore, Jpn. J. Appl. Phys. 24 (Suppl. 24-2) (1985) 727.
[12] Ya.V. Burak, V.T. Adamiv, I.M. Teslyuk, V.M. Shevel, Rad. Meas. 38 (2004) 681.
[13] V.T. Adamiv, Ya.V. Burak, I.V. Kityk, J. Kasperczyk, R. Smok, M. Czerwinski, Opt. Mater. 8 (1997) 207.
[14] Y. Losovyj, I. Ketsman, E. Morikawa, Z. Wang, J. Tang, P. Dowben, Nucl. Instrum. Methods Phys. Res. A 582 (2007) 264.

[15] P.A. Dowben, D. LaGraffe, M. Onellion, J. Phys. Condens. Matter 1 (1989) 6571.
[16] J. Hormes, J.D. Scott, V.P. Suller, Synchrotron Radiat. News 19 (2006) 27.
[17] D. Wooten, I. Ketsman, J. Xiao, Ya.B. Losovyj, J. Petrosky, J. McClory, Ya.V. Burak, V.T. Adamiv, P.A. Dowben, in: D.L. Perry, A. Burger, L. Franks, K. Yasuda, M. Fiederle (Eds.), Nuclear Radiation Detection Materials, Mater. Res. Soc. Symp. Proc., vol. 1164, 2009, L04-04.
[18] D. Wooten, I. Ketsman, Jie Xiao, Ya.B. Losovyj, J. Petrosky, J. McClory, Ya.V. Burak, V.T. Adamiv, P.A. Dowben, Physica B 405 (2010) 461.
[19] M.M. Islam, V.V. Maslyuk, T. Bredow, C. Minot, J. Phys. Chem. B 109 (2005) 13597.
[20] A.Yu. Kuznetsov, A.V. Kruzhalov, I.N. Ogorodnikov, A.B. Sobolev, L.I. Isaenko, Phys. Solid State 41 (1999) 48.
[21] N.V. Smith, Rep. Prog. Phys. 51 (1988) 1227.
[22] G.I. Malovichko, V.G. Grachev, A.O. Matkovskii, Sov. Phys. Solid State 33 (1991) 1107.
[23] Ya.V. Burak, B.V. Padlyak, V.M. Shevel, Rad. Effects Defects Solids 157 (2002) 1101.
[24] A.A. Sehery, D.J. Somerford, J. Phys. Condens. Matter 1 (1989) 2279.
[25] W.H. Brattain, J. Bardeen, Bell Syst. Tech. J. 32 (1953) 1.
[26] D.K. Schroder, Meas. Sci. Technol. 12 (2001) R16.
[27] J.E. Demuth, W.J. Thompson, N.J. DiNardo, R. Imbihl, Phys. Rev. Lett. 56 (1986) 1408.
[28] M. Alonso, R. Cimino, K. Horn, Phys. Rev. Lett. 64 (1990) 1947.
[29] K. Stiles, A. Kahn, Phys. Rev. Lett. 60 (1988) 440.
[30] C.-S. Kim, J.-H. Park, B.K. Moon, H.-J. Seo, B.-C. Choi, Y.-H. Hwang, H.K. Kim, J.N. Kim, J. Appl. Phys. 94 (2003) 7246.